Received: 17 February 2023 | Revised: 17 March 2023 | Accepted: 21 March 2023

DOI: 10.1002/hipo.23534

RESEARCH ARTICLE

WILEY

View cells in the hippocampus and prefrontal cortex of macaques during virtual navigation

Benjamin W. Corrigan[1] | Roberto A. Gulli[2,3] | Guillaume Doucet[4,5] | Borna Mahmoudian[1] | Mohamad Abbass[6] | Megan Roussy[1,7] | Rogelio Luna[1,8] | Adam J. Sachs[4] | Julio C. Martinez-Trujillo[1,9,10]

[1]Department of Physiology and Pharmacology, University of Western Ontario, London, Ontario, Canada

[2]Zuckerman Mind Brain Behavior Institute, Columbia University, New York, New York, USA

[3]Center for Theoretical Neuroscience, Columbia University, New York, New York, USA

[4]The Ottawa Hospital, University of Ottawa, Ottawa, Ontario, Canada

[5]Realize Medical, Ottawa, Ontario, Canada

[6]Western University Department of Clinical Neurological Sciences, London Health Sciences Centre, Western University, London, Ontario, Canada

[7]National Science and Engineering Research Council, Ottawa, Ontario, Canada

[8]Facultad de Medicina y Ciencias Biomédicas, Universidad Autónoma de Chihuahua, Chihuahua City, Mexico

[9]Department of Psychiatry, Schulich School of Medicine and Dentistry, University of Western Ontario, London, Ontario, Canada

[10]Western Institute for Neuroscience University of Western Ontario, London, Ontario, Canada

Correspondence
Julio C. Martinez-Trujillo, Department of Physiology and Pharmacology, University of Western Ontario, London, ON, Canada.
Email: julio.martinez@robarts.ca

Funding information
Canadian Institutes of Health Research; McGill David G. Guthrie Fellowship; National Science Foundation, Grant/Award Number: 2015276; Natural Sciences and Engineering Research Council of Canada; Ontario Graduate Scholarships; The Deutsche Forschungsgemeinschaft; Jonathan & Joshua Memorial Graduate Scholarship in Mental Health Research; BrainsCAN

Abstract

Cells selectively activated by a particular view of an environment have been found in the primate hippocampus (HPC). Whether view cells are present in other brain areas, and how view selectivity interacts with other variables such as object features and place remain unclear. Here, we explore these issues by recording the responses of neurons in the HPC and the lateral prefrontal cortex (LPFC) of rhesus macaques performing a task in which they learn new context-object associations while navigating a virtual environment using a joystick. We measured neuronal responses at different locations in a virtual maze where animals freely directed gaze to different regions of the visual scenes. We show that specific views containing task relevant objects selectively activated a proportion of HPC units, and an even higher proportion of LPFC units. Place selectivity was scarce and generally dependent on view. Many view cells were not affected by changing the object color or the context cue, two task relevant features. However, a small proportion of view cells showed selectivity for these two features. Our results show that during navigation in a virtual environment with complex and dynamic visual stimuli, view cells are found in both the HPC and the LPFC. View cells may have developed as a multiarea specialization in diurnal primates to encode the complexities and layouts of the environment through gaze exploration which ultimately enables building cognitive maps of space that guide navigation.

KEYWORDS
hippocampus, non-human primate, prefrontal cortex, view cells, virtual environment

1 | INTRODUCTION

In many species of diurnal primates, the ability to orient gaze toward regions of visual space is of critical importance to sample detailed information about the environment. Directing gaze allows for exploring objects and space from a distance (far sensing), without the need to visit the corresponding locations. This process may be different in nocturnal animals with poor vision such as rats and mice relying on "near" sensory adaptations such as whiskers to explore the environment. Indeed, nocturnal rodents frequently visit spatial locations during exploratory behaviors, and hippocampal (HPC) place cells encode the location they are visiting (O'Keefe & Nadel, 1978). Interestingly, in diurnal primates such as macaque monkeys, previous studies have reported cells in the HPC that selectively respond to specific views of a scene (De Araujo et al., 2001; Mao et al., 2021; Robertson et al., 1998; Rolls & O'Mara, 1995). Whether view cells exist in other brain regions and how they interact with encoding of place and visual features remains unclear.

There have been two main experimental approaches to studying how HPC neurons respond during the viewing of scenes: (1) presenting stimuli at different locations on a monitor(s) or in spatial windows that experimenters can control, and assessing neuronal responses when gaze is directed to the stimuli (Cahusac et al., 1989; Feigenbaum & Rolls, 1991; Nowicka & Ringo, 2000; Rolls et al., 1989; Tamura et al., 1990, 1992), and (2) monitoring what is visible to the subject while it moves or is moved around a room and correlating the view with neuronal responses (Georges-François et al., 1999; Ono et al., 1993; Robertson et al., 1998; Rolls & O'Mara, 1995). The first method led to the discovery of hippocampal neurons that responded when gaze was directed at specific locations on the screen, or to different screens. These experiments found proportions of gaze position selective neurons to range from 4% to 23%. In general, these experiments are not able to differentiate between egocentric and allocentric encoding since animals and environments remain stationary. Feigenbaum and Rolls (1991) were able, for a subset of neurons, to move the monkey in relation to the screens, or the screen in relation to the monkey and reported mainly allocentric but some egocentric neuronal responses. In subsequent experiments where monkeys were moved or freely locomoted around a room while recordings were carried out, some neurons were found to respond when animals looked at a particular part of the environment. These responses were relatively invariant with respect to the place where the macaque was located, to head direction, or to eye position. These neurons with allocentric view responses were termed "spatial view cells" (Rolls, 2022; Rolls et al., 1998; Rolls & O'Mara, 1995).

Some studies have used virtual reality to simulate complex visual scenes in naturalistic conditions and trained monkeys to navigate virtual mazes using a joystick. Virtual environments allow experimental manipulation of object features and task contingencies to determine how important each constituent part might be. While there have been several studies that have used virtual environments to explore hippocampal encoding (Doucet et al., 2020; Gulli et al., 2020; Hori et al., 2005; Miller et al., 2013; N. Sato et al., 2004), few have included gaze in their analyses. Furuya et al. (2014) used a virtual environment where the monkey freely navigated, but only binned heading direction to get an approximation of view, similar to Rolls and O'Mara (1995). Wirth et al. (2017) made use of a virtual environment while recording gaze position, and found cells that responded during gaze directed at a specific landmark. However, this frequently depended on the virtual position and trajectory in the maze.

In the current study, we examine whether and how neurons in the HPC and lateral prefrontal cortex (LPFC) of macaque monkeys encode view and other related variables. We used a task set in a virtual environment (Gulli et al., 2020) and recorded from either the HPC or LPFC of rhesus macaques while they navigated the environment using a joystick. Eye position was monitored using video-based eye tracking. The X-maze consisted of a corridor that branches out at the two ends. At either end, the monkey made a two-alternative forced choice between two colored discs. The animal had to navigate to a disc to obtain the associated reward. The rewarded disc was determined by the context, a texture applied to the maze walls (e.g., wood walls mean the target is a blue disc, steel walls mean the target is a red disc). Because the set of discs' colors changed every session/day, the monkey would have to associate the context and the color to perform the task above chance level. Through various dissociations, we were able to assess virtual view selectivity as well as the effects of virtual position in the maze and of changing task relevant visual features. We found view cells in both areas. A proportion of these cells also encoded visual features and view position (north vs. south) in the maze.

2 | METHODS

2.1 | Subjects

We used four male rhesus macaques (*Macaca mulatta*), at two different facilities. Monkey R (14 years old, 12 kg) and Monkey W (7 years old, 7 kg) were cared for at the McGill Comparative Medicine and Animal Resources Centre. They were used in the hippocampal (HPC) experiments. Monkey T (10 years old, 12 kg) and Monkey B (9 years old, 10 kg) were cared for under the Animal Care and Veterinary Services at Western University. They were used in the lateral prefrontal cortex (LPFC) experiments. All handling and procedures were carried out in accordance with Canadian Council for Animal Care Guidelines and approved by either the McGill University Animal Care Committee

(Monkeys R and W) or the Western University Animal Care Committee (Monkeys T and B).

2.2 | Surgical procedures

Hippocampal surgeries: These are fully described in Gulli et al. (2020), but briefly, a presurgical MRI was acquired at 500 µm isotropic (T1-weighted with 3T strength) and used for skull reconstruction and neuronavigation (BrainSight, Rogue Research, QC, Canada). With a skull reconstruction, a titanium headpost was planned and custom built, and hippocampal chamber placement was also planned over the right prefrontal cortex, targeting the mid to posterior hippocampus with trajectories perpendicular to the long and transverse axes. To place these, two surgeries were carried out under general anesthesia, separated by a minimum 8-week recovery period. A post-operative CT scan was used to verify the chamber trajectory, using cannulas situated in the chamber grid, which was then co-registered to the MRI. This allowed for precise trajectory and depth mapping for each grid hole. Trajectory end points are illustrated in Figure 1e.

Prefrontal surgeries: Custom-designed PEEK head cap surgeries are fully described in Blonde et al. (2018). Briefly, a 7T T1 MRI was acquired at 350 µm isotropic for Monkey T and 400 µm isotropic for monkey B, and a PEEK head cap was custom designed to fit the skull that allowed for targeted craniotomies, a headpost, and attachment of Cereport connections (Blackrock Neurotech, Salt Lake City, UT, USA). This was implanted under general anesthesia. After a minimum 8-week recovery period, again under general anesthesia, two 96-channel Utah arrays (Blackrock Neurotech, Salt Lake City, UT, USA) were implanted into the dorsal and ventral aspects of area 9/46 in the left hemisphere of the LPFC (see Figure 1f for examples).

2.3 | Experimental setup

Monkeys were seated and head fixed in a custom primate chair in front of a computer monitor (eye-screen distance: 80 cm; viewing angle: 32° × 24° visual angle (DVA); resolution: 1280 × 1024) with a 75 Hz refresh rate. A two-axis joystick (M212, PQ Controls, Bristol, CT, USA) was attached to the chair for navigation in virtual environment tasks. The position of the left eye was tracked via video-oculography (EyeLink 1000, SR Research, Ottawa, ON, Canada) at 500 Hz. A juice reward was given based on trial performance (Figure 1a).

The virtual environment tasks were generated using a video game engine (Unreal Engine 3, Epic Games Inc., Potomac, NC, USA) running on a dedicated computer. The position in the environment of every frame was recorded and transferred to the experimental control computer via network link. The experimental control computer was running a custom MATLAB (Mathworks Inc., Natick, MA, USA) experiment control suite that tracked task progression and aligned visual stimuli and gaze with the neural data.

2.4 | Task

There were two variants of the virtual reality task, which both took place in the X-maze: a corridor with a "Y" at either end where two colored discs would appear (Figure 1b). In this task, the monkeys performed a series of two-alternative forced choice trials, where they decided to collect one of two colored discs. The rewarded choice was determined by the context, which was cued using one of two textures applied to the maze walls (wood or steel) (Video S1). The reward was chosen based on the context, such that if the colors were blue and green, blue would be rewarded in "wood" (context 1) and green would be rewarded on "steel" (context 2) trials. For the LPFC experiments, the monkeys had only two potential colors (high and low reward). Monkeys R and W had a slight variation, described in Gulli et al. (2020) that had three possible colors (high, middle and low rewards, Figure 1c). For this paper, we only analyzed foveations on the high and low reward value objects, so the value of objects foveated was like the other task.

2.5 | Eye movements processing

Eye movement classification is described in Corrigan et al. (2017). Briefly, we used an acceleration threshold to find potential saccadic periods, took the peak velocity of this period, and looked at the linearity of the signal going forward until it stopped being linear to find the end point (same thing moving backwards from the peak to find the start point). Inter-saccade foveation periods were also separated into smooth pursuits and fixations based on linearity and movement characteristics but were all treated as "foveations" for this paper.

2.6 | Recording

Hippocampal units were recorded in monkeys R and W and are the same as described in (Gulli et al., 2020). Briefly, 1–4 high impedance electrodes were lowered per day to the hippocampus via MRI-verified grid positions, and signals were recorded on a neural signal processor (Cerebus, Blackrock Neurotech, Salt Lake City, UT, USA) and neural signals were high-passed at 250 Hz. The LPFC recordings were done using two 96-channel microarrays per animal (Utah array, Blackrock Neurotech, Salt Lake City, UT, USA), and were processed the same way as the HPC recordings. Waveforms were sorted offline using Plexon Offline Sorter (Plexon, Dallas, TX, USA). HPC units were all manually sorted. LPFC units were sorted using a combination of automated and manual spike sorting techniques.

2.7 | Analysis

To assess task performance, we computed performance during periods of the task where animals reached a stable level of performance: a 50-trial window near the end of the session. For the

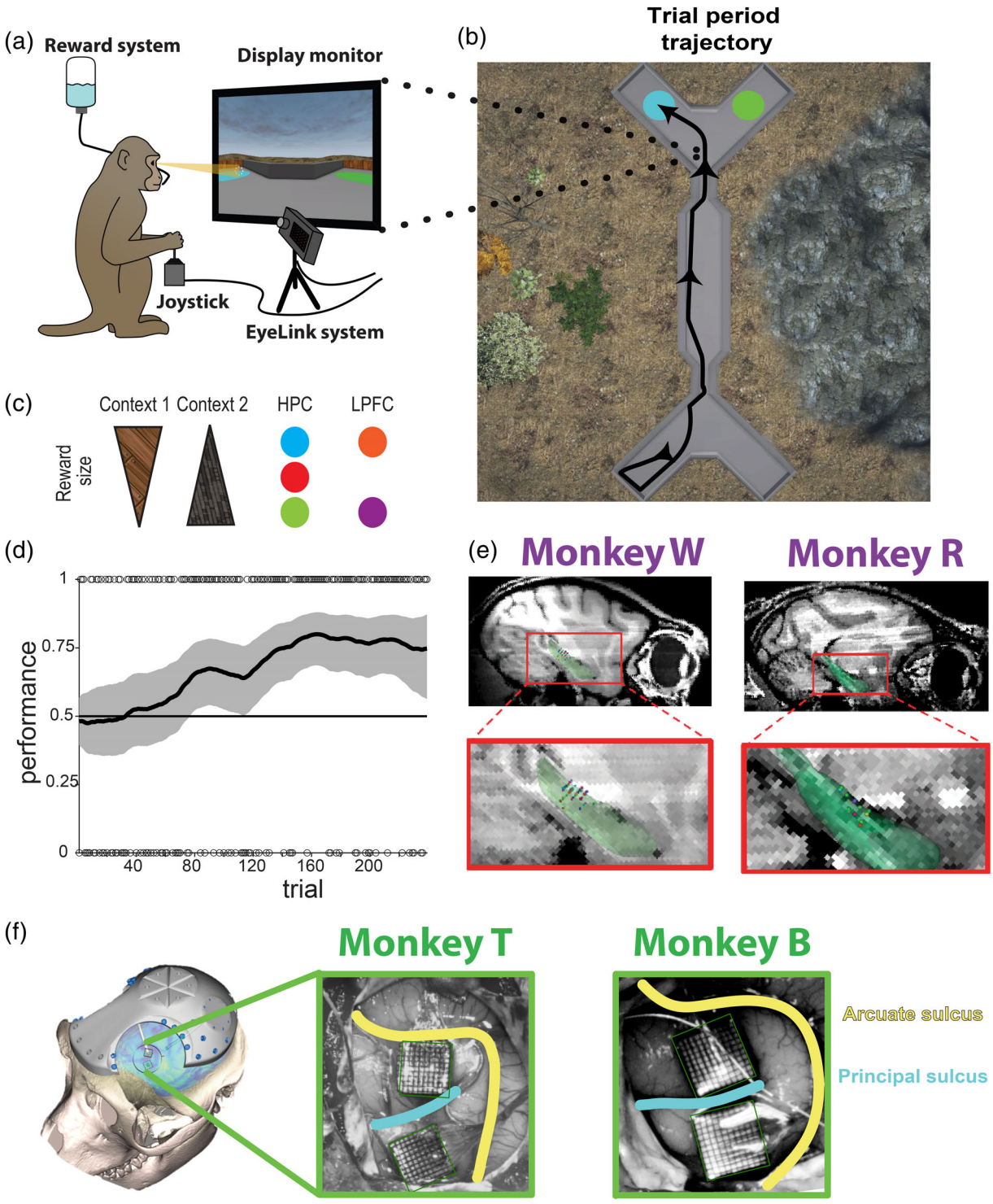

FIGURE 1 Monkeys performed a context-object association task in a virtual environment while we recorded from either the HPC or LPFC. (a) Monkey set-up where they used a two-axis joystick to navigate the virtual environment displayed on the screen. (b) An overhead view of the virtual environment with an example trial trajectory. (c) Example reward hierarchies for HPC and LPFC. Colors were changed each day. (d) Example performance estimation curve with confidence intervals of whether the rule is learned (when the confidence intervals do not intersect with chance of 50%). (e) Recording locations at trajectory end points in right, mid to posterior HPC. (f) Microelectrode array locations in left LPFC.

example learning curve in Figure 1d, we used the method from Smith et al (2004) which predicts when performance is no longer at chance.

To assess view encoding during the decision period where we could also measure effects of changing different features of the view, we first had to determine whether our recorded units in either area

were selective for the virtual view, and not simply selective for eye-in-head or gaze-on-screen position. The first two foveations on either object in the decision period were stereotyped in that 99% of these fixations fell within rectangles with limits between 6 and 14 DVA in the X dimension and −5 and 0 DVA in the Y dimension on the right side, and the same dimension on the left, but with negative *X* values (−14 and −6 DVA). We compared firing rates during foveations on these screen locations during the decision period, and then measured selectivity for firing rates during foveations on the same screen locations during navigation. Firing rates were calculated based on the duration of the foveation (number of spikes that occurred during the foveation divided by the duration). Firing rate selectivity was determined using a rank-sum test and a permutation test with 1000 shuffles. For the foveations in the decision period, we used the first foveation on either side that started after object appearance. Foveations that did not end during the decision period were excluded.

Because there were two positions in the maze where a decision had to be made (i.e., one at the north and south ends of the X-maze), we also wanted to assess whether view selectivity was modulated by which end the monkey was at. To do this, we used a generalized linear model (GLM) with a log link function as the hippocampal firing rates were frequently 0 Hz and approximated a Poisson distribution rather than a Gaussian distribution. We used two variables, a virtual view (i.e., left vs. right arm of maze), and the virtual position at either the north or south decision point (Figure 4a). To assess significance, we first fit a model (Equation 1) that contained the two variables and their interaction.

$$ln(y) = \beta_0 + \beta_1{}^{*}\text{virtual view} + \beta_2{}^{*}\text{virtual position} + \beta_3{}^{*}\text{virtual view}{}^{*}\text{virtual position} \quad (1)$$

We used a deviance test to determine whether the model was a better fit than a constant with a $p < 0.05$. If the fit was significant, we performed a coefficient test for each variable, where we evaluated the βs for both the variable and the interaction together. We then evaluated the interaction β separately. Finally, we used a permutation test by shuffling the labels of each foveation 5000 times and rerunning the regression and coefficient tests. We considered a test result significant if the original *p*-value was lower than at least 95% of the permuted *p*-values.

There were two variables that changed within a virtual view on a particular side that were both task-relevant: the color of the object and the context cue texture on the wall at the end of the maze. To analyze the effect of changing either of these variables, we again used a GLM to assess unit selectivity for the virtual view and color (Equation 2) or context (Equation 3) separately. We used the same methods used in the location analysis.

$$ln(y) = \beta_0 + \beta_1{}^{*}\text{virtual view} + \beta_2{}^{*}\text{color} + \beta_3{}^{*}\text{virtual view}{}^{*}\text{color} \quad (2)$$

$$ln(y) = \beta_0 + \beta_1{}^{*}\text{virtual view} + \beta_2{}^{*}\text{context} + \beta_3{}^{*}\text{virtual view}{}^{*}\text{context} \quad (3)$$

3 | RESULTS

We trained four monkeys (*Macaca mulatta*) to navigate in a virtual environment and perform an associative learning task (Video S1). We recorded from neurons in the right hippocampus (HPC) of two animals and from the left lateral prefrontal cortex (LPFC, area 9/46) of the other two animals. During task trials, the animal used a joystick to navigate from one end of the maze to another (Figure 1a,b). When the monkey reached the point where two arms branched (the decision point), two colored discs appeared. The monkey then navigated to one of the discs (the target). Once the animal reached the target, a liquid reward was delivered. The size of the liquid reward was based on a reversed context-dependent hierarchy. The context was defined by the texture of the walls (wood vs. steel) (Figure 1c). For the HPC experiments, three color discs were used during each session corresponding to high, middle, and low rank values (relative reward values 100%, 50%, and 0%, respectively), depending on the context. In a session, new colors were selected pseudo-randomly, ensuring that colors were not repeated from the preceding session. We limited the analyses of HPC data to the highest and lowest ranked colored discs. Animals learned the task (Figure 1d) with mean performance over a 50-trial window of 75.8% (monkey W) and 61.3% (monkey R) for the HPC monkeys. For the LPFC monkeys, the average performance was 85.3% (monkey B) and 74.5% (monkey T).

3.1 | View selective neurons in the HPC and LPFC

We included in our analyses 37 sessions (7 with monkey R, 30 with monkey W) and recorded from 226 units in the right mid to posterior HPC (Figure 1e), 34 units in monkey R and 192 in monkey W, using 1–4 single electrodes. For the LPFC, we used Utah microelectrode arrays in the left LPFC (Figure 1f) and recorded 435 units in monkey B and 281 units in monkey T using two sessions from each (total of 716 units).

To assess foveations, we first classified the eye signal into saccades (including post-saccadic oscillations) and foveations, comprised of fixations and smooth pursuits (Figure 2a–c; see methods and Corrigan et al., (2017)). During the decision period, the monkeys mostly only directed their gaze at the two discs, so we were able to define one rectangle on either side that contained 99% of the foveations (Figure 2c,d upper). We treated these as two specific virtual views. To create a control comparison for gaze-on-screen, we collected all the foveations that occurred in the same windows in screen coordinates while the monkey moved through the navigation area (Figure 2d lower), before it reached the decision point and when the discs were not visible.

Some individual neurons in both the HPC (Figure 3a) and the LPFC (Figure 3b) respond differentially after foveation onset while the animal held the same gaze position on the screen during navigation (left panel) and decision (right panel). In both example units shown in the figure, the responses when foveating on the left or right region of

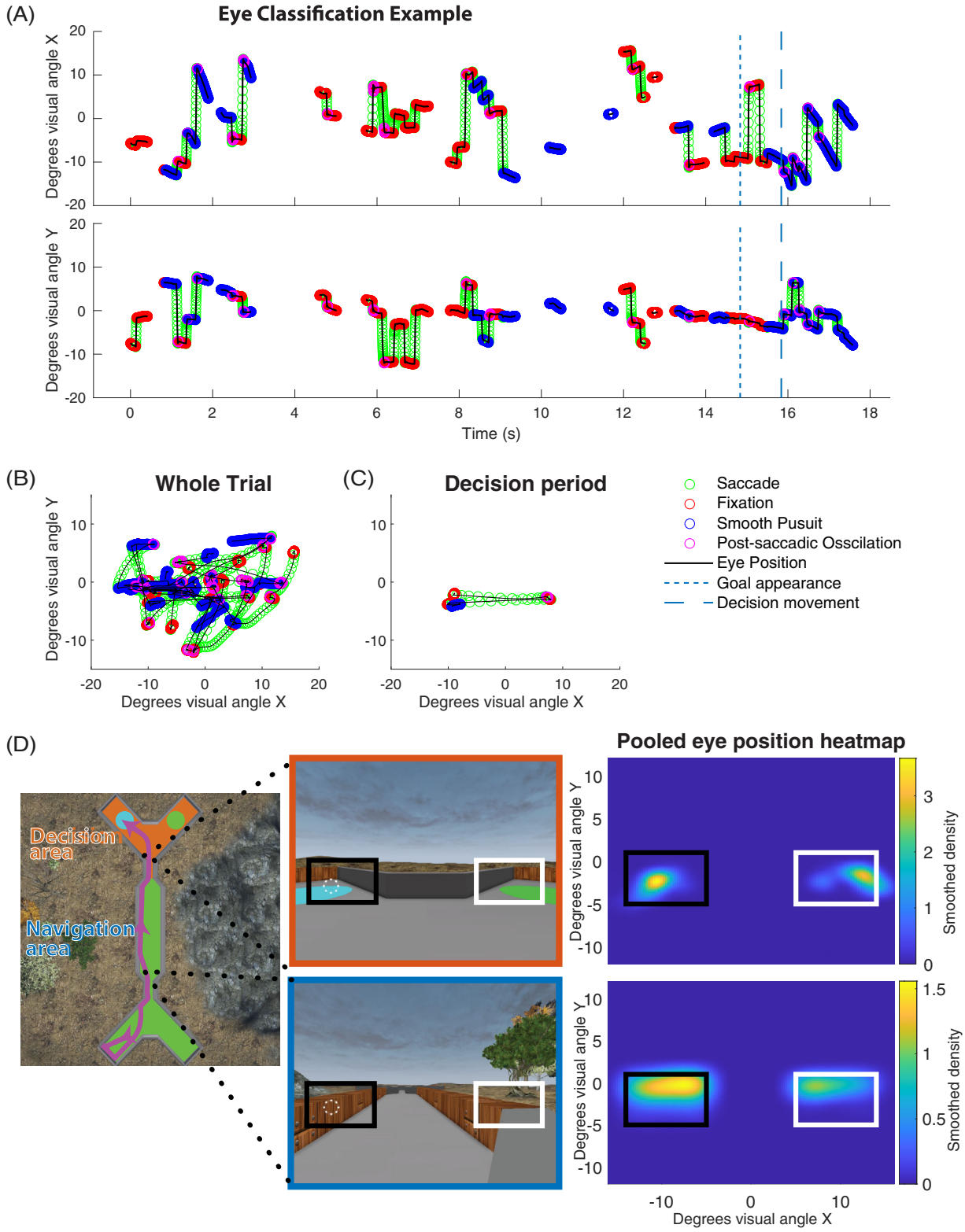

FIGURE 2 Eye position was classified, and foveations were selected from specific screen locations. (a) Example eye position traces separated into X and Y components and classified into saccades, and two types of foveations, fixations and smooth pursuits, as well as post-saccadic oscillations. (b) The same trial as in A, but plotted in screen coordinates. (c) Same as (b), but only the decision period is plotted. (d) A layout of the maze, with two example frames from two different locations in the maze: at the decision point (above) with two rectangles delimiting where 99% of the foveations during the decision period fell on the screen, and during navigation in the corridor (below) with the same rectangles. To the right are heat maps of foveation locations during the decision period and foveation locations during navigation that fell within the two rectangles from an example session for monkey W (HPC) and monkey B (LPFC).

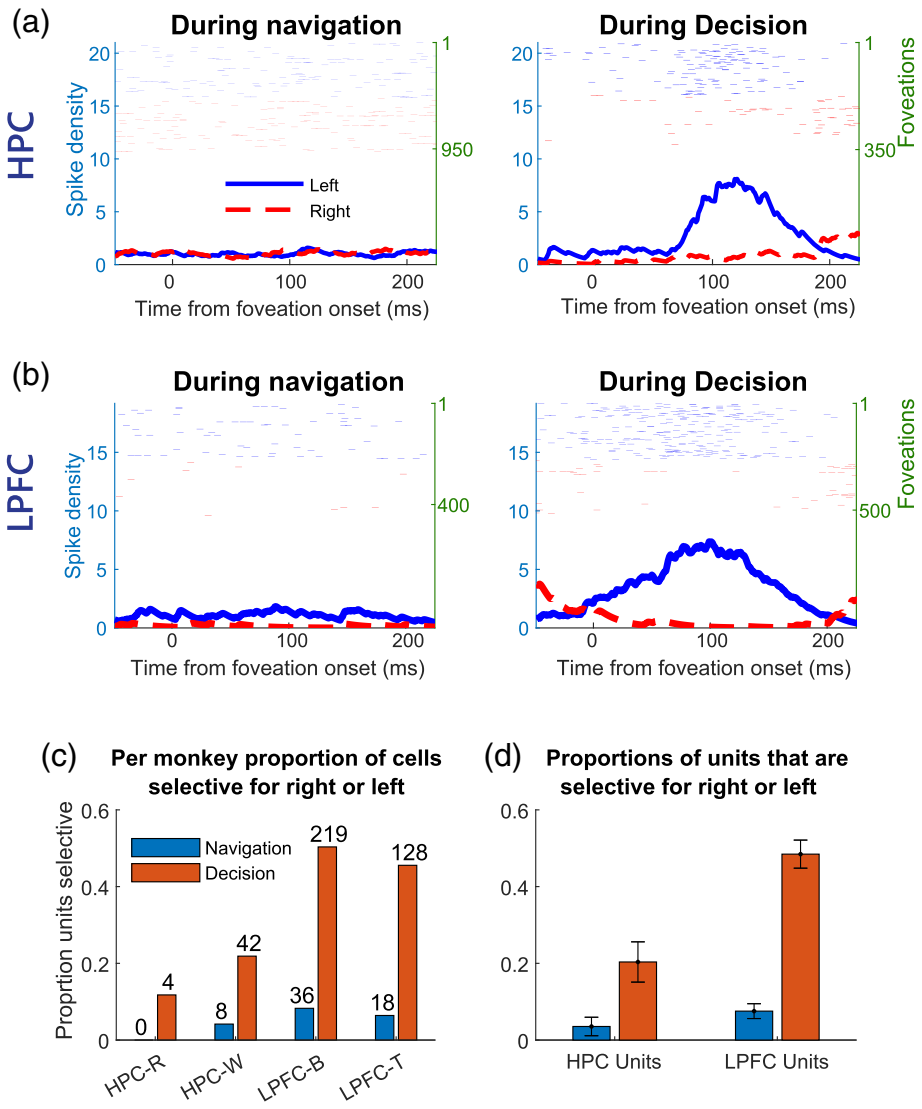

FIGURE 3 Units in both regions are more responsive to virtual view at decision point than the screen location during the navigation period. (a) HPC example unit that is selective for foveations on the left, but only during the decision period. (b) LPFC example unit that is selective for foveations on the left, but only during the decision period. (c) Proportion of units for each monkey that are selective for screen locations during navigation or decision, actual counts are written above each bar. Monkey initial and recorded area are indicated. (d) Proportions of units selective for screen location during navigation or decision for each area with 95% confidence intervals.

the screen were the same during navigation, but responses differed during the decision period. The main change in firing rate was an increase in one of the conditions (gaze directed left for the HPC example unit and gaze directed right for the LPFC example unit). To quantitatively assess selectivity in each neuron, we calculated a neuron's firing rate during foveations in the navigation (gaze-on-screen positions) and decision (end of maze and discs views) periods. For each period, we compared the rates between left and right sides of the screen using a rank-sum test, calculating significance with a permutation test with 1000 shuffles. Monkey R had no significant units for screen position during the navigation period (0/34), while 4.2% (8/192) of monkey W's neurons showed screen position selectivity (Figure 3c). In contrast, during the decision period, 11.8% (4/34) of Monkey R's neurons and 21.9% (42/192) of monkey W's neurons were selective for the virtual view (Figure 3c). For the whole hippocampal population, only 3.5% (±2.4% CI) were significant for screen side during the navigation period. During the decision period, a total of 20.4% (±5.3% CI) of neurons were selective (Figure 3d), approximately 6 times the proportion found during the navigation period. This difference was statistically significant (95% confidence intervals for proportion do not overlap).

For the LPFC, 8.3% (36/435) of monkey B's units and 6.4% (18/281) of monkey T's units were selective for screen side during the navigation period, while 50.3% (219/435) of monkey B's units, and 45.5% (128/281) of monkey T's units were selective for the virtual view during the decision period (Figure 3c). In total, 7.5% (±1.9% CI) were selective during navigation and 48.5% (±3.7% CI) during the decision period (Figure 3d). Again, these differences were statistically significant (95% confidence intervals for proportions do not overlap, Figure 3c). Thus, in both areas the proportion of selective units was higher during the decision relative to the navigation period. These results indicate that the view rather than the gaze-on-screen position was driving the selectivity of the units.

3.2 | View selectivity at the maze ends

The view of the maze was similar (although not identical) in the north and south decision points (see views screenshots in Figure S1). In our

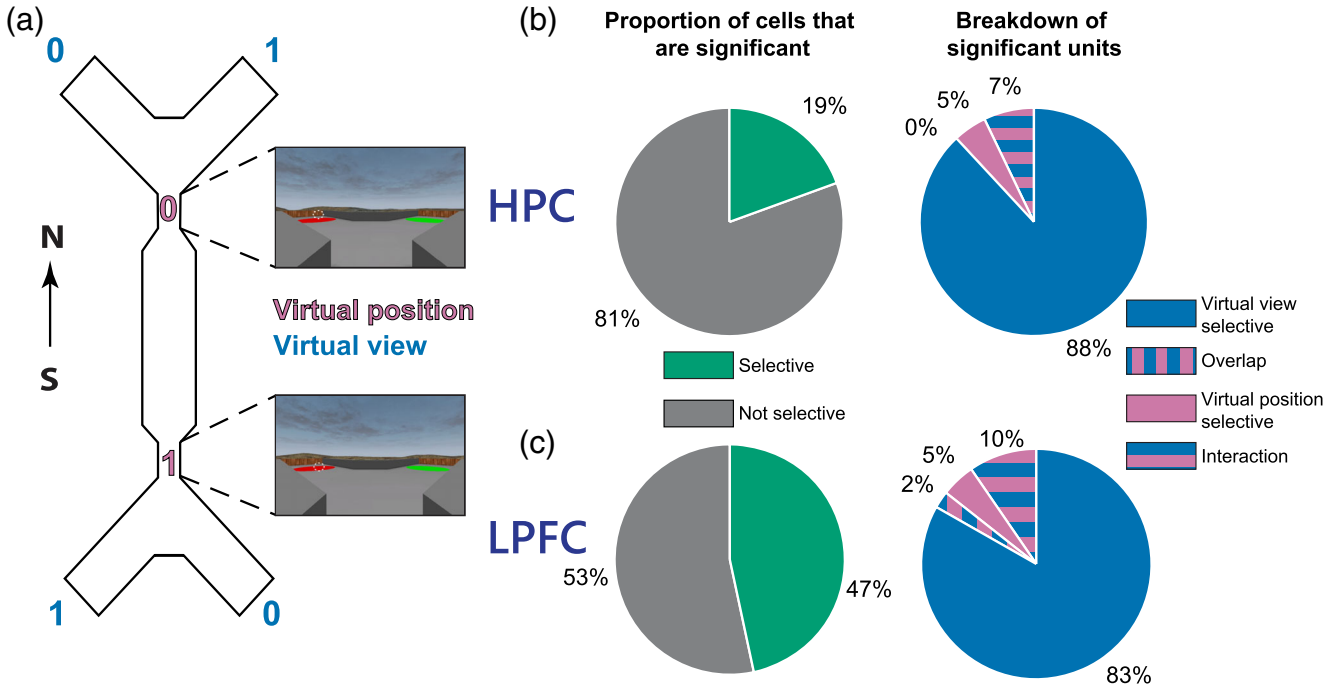

FIGURE 4 Most units selective for virtual view are unaffected by which virtual position (north or south end of maze) the virtual view is acquired. (a) An illustration of the binary coding of virtual position and virtual view, with example views demonstrating the small variances in distal features at the two maze ends. (b) The proportion of units where any beta is significant using a GLM with betas for virtual position, virtual view, and their interaction in the HPC. To the right are the specific proportions of significant units for either main effect, an interaction, or an overlap, where both main effects are significant, but not the interaction. (c) Same as (b), but for the LPFC.

previous analyses, we pooled north and south ends of the maze. However, there were cues that could have been used to distinguish north and south along the navigation path (e.g., mountain on one side of the maze, and trees on the other). Although they were not visible at the decision points (Figure S1), it is possible the animals oriented themselves in the environment and that neurons in the HPC and LPFC encoded that information. We should clarify there was no clear use to this distinction, but we must remain aware of the possibility the animal may have done it. To explore this issue, we used a generalized linear model (GLM) with a log link function (Equation 4) and a coefficient test assessed for significance with a permutation test.

$$ln(y) = \beta_0 + \beta_1{}^{*}\text{virtual view} + \beta_2{}^{*}\text{virtual position} + \beta_3{}^{*}\text{virtual view}{}^{*}\text{virtual position} \quad (4)$$

We only used units that had at least 20 foveations of each combination of virtual view and virtual position (e.g., virtual position north and virtual view to the right, Figure 4c). In the HPC, 19.4% (±5.3%, 95% CIs) of units show significance for one of the two binary variables: maze virtual position (north vs. south) and virtual view (left vs. right) (Figure 4a,b). Of the units that were significantly modulated, most were selective for virtual view to the left or right (95.2% ±6.4% CIs), either through a main effect or interaction. A significantly smaller percentage were modulated by virtual position, north or south (11.9% ±9.8% CIs). Of the selective units, 88.1% (±9.8% CIs) were selective only for virtual view, and 4.8% (±6.4% CIs) were selective only for virtual position. 7.1% (±7.8% CIs) show an interaction between virtual view and virtual position. Thus, virtual view was the predominant form of selectivity in these units (non-overlapping 95% CIs for proportions).

For the LPFC, 46.7% (±3.7% CIs) of units were selective for at least one variable. Again, most units were selective for virtual view (95.2% (±2.3% CIs)) and a smaller proportion were selective for virtual position (16.8% (±4.0% CIs)). Of the selective units, 83.2% (±4.0% CIs) were selective for virtual view only, while 4.8% (±2.3% CIs) were selective for virtual position only. 2.4% (±1.6% CIs) of units had a non-interacting overlap, while 9.6% (±3.2% CIs) had an interaction between virtual view and position. As the virtual view selectivity was predominant in both areas, all further analyses focus on virtual views to the left or right and ignore virtual position.

3.3 | Selectivity for object features

In our design two different non-spatial features were used, the color of the discs and the context texture. We found some individual neurons in both regions that responded differentially to the different colors (Figure 5a), or to the different context cues (Figure 5b). We explored whether selectivity for these features interacted with virtual view selectivity by repeating the previous GLM analyses. First, using virtual view and object color according to Equation 5.

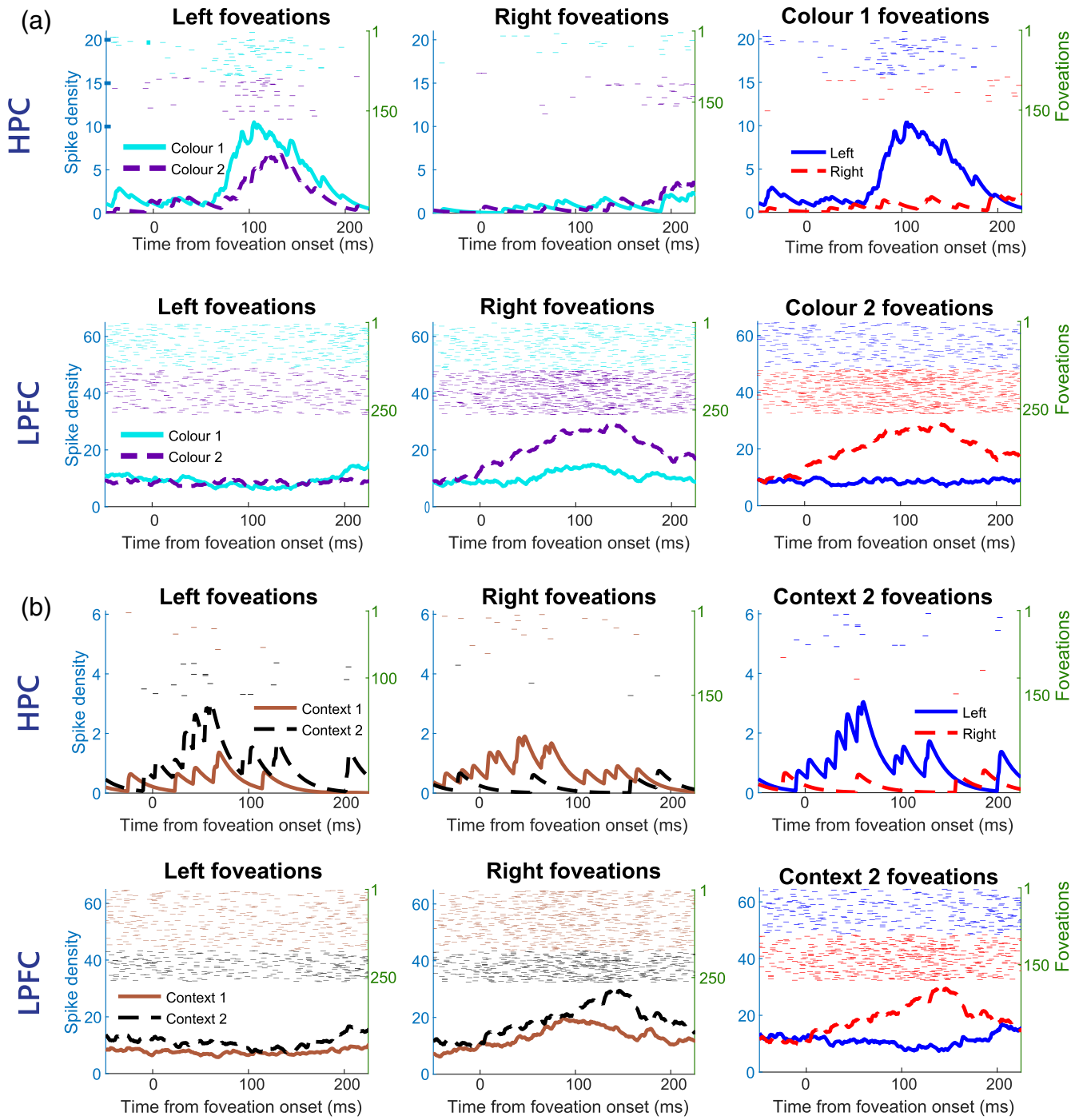

FIGURE 5 Example units where there is selectivity for virtual view and a visible feature. (a) Example rasters and spike density functions for units selective for a color in HPC (upper) and LPFC (lower). The first two columns are foveations on the left or right respectively, and the third column is a comparison of left and right foveations on the color that the example neuron is selective for. (b) Same as (a), but for context and virtual view.

$$ln(y) = \beta_0 + \beta_1{}^{*}\text{virtual view} + \beta_2{}^{*}\text{color} + \beta_3{}^{*}\text{virtual view}{}^{*}\text{color} \quad (5)$$

We excluded units with fewer than 20 foveations for each combination of virtual view and object color. For the HPC, 25.5% (±5.8% CIs) of units were significant for at least one factor (Figure 6a). Again, most were significant for virtual view at 98.2% (±3.5% CIs), and almost a third were selective for color at 32.7% (±12.4% CIs). Of these selective units, 67.3% (±12.4% CIs) were only selective for virtual view, and only 1.8% (±3.5% CIs) were selective only for color. Another 1.8% (±3.5% CIs) show a non-interacting overlap, while 29.1% (±12.0% CIs) show an interaction between color and virtual view.

Results were similar for the LPFC (Figure 6a lower), where 48.9% (±3.7% CIs) were significant for at least one factor, of which 92.0% (±2.8% CIs) were significant for virtual view and 40.0% (±5.1% CIs)

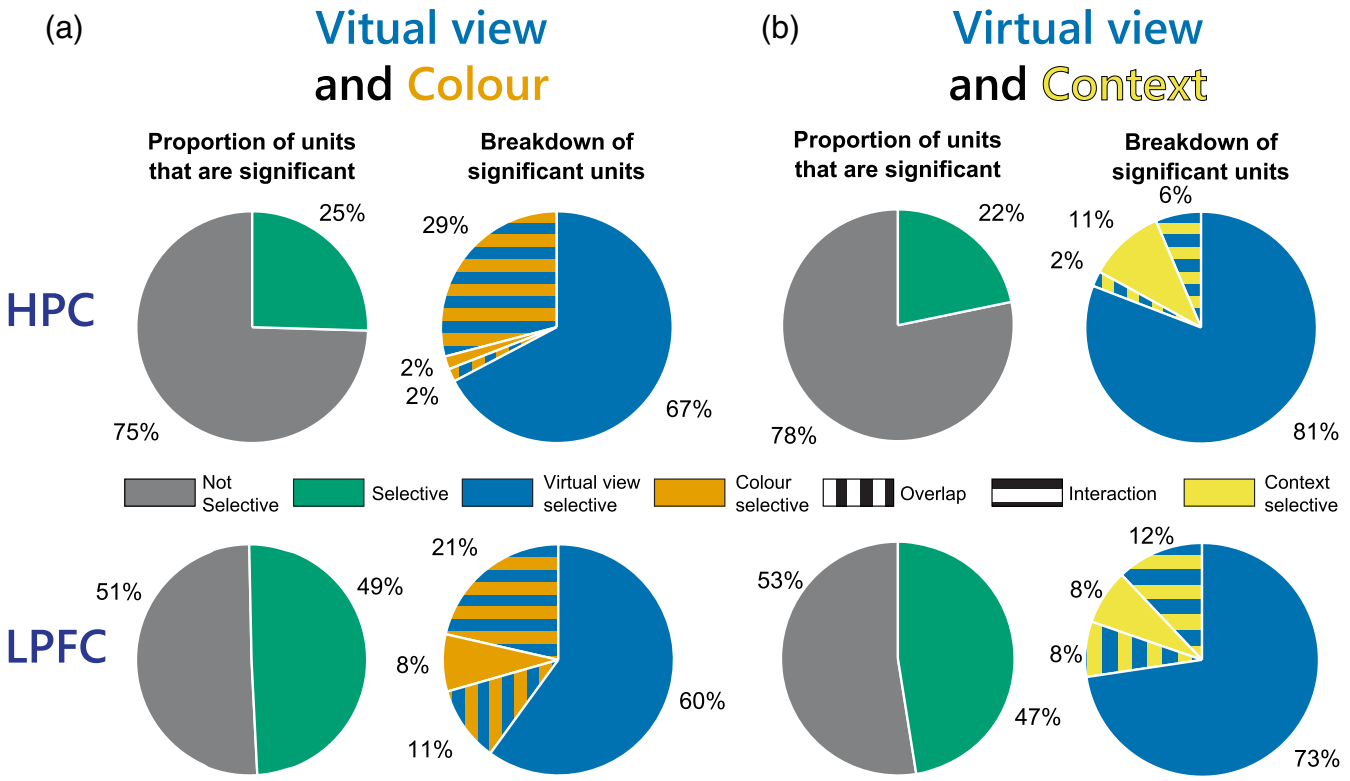

FIGURE 6 Virtual view selective cells can also be selective for visual features of object color and context cues. (a) Proportions of units with any significant betas for virtual view, color or an interaction (left) as well as the breakdown for those units (right) in the HPC (upper) and LPFC (lower). (b) Same as (a), but for the models with virtual view and context.

were significant for color. 60.0% (±5.1% CIs) were only selective for virtual view, 8.0% (±2.8% CIs) were only selective for color, 10.6% (±3.2% CIs) show a non-interacting significant main effect for each factor, and 21.4% (±4.3% CIs) show an interaction between color and virtual view. Again, in both regions there was a significantly higher percentage of units that were selective for virtual view than for color (non-overlapping 95% CIs for proportions).

The other variable that changed in the virtual view was the texture on the wall of the maze that indicated the context. We used Equation 6 to explore the interaction between context/texture and virtual view.

$$ln(y) = \beta_0 + \beta_1{}^{*}\text{virtual view} + \beta_2{}^{*}\text{context} + \beta_3{}^{*}\text{virtual view}{}^{*}\text{context} \quad (6)$$

Repeating the previous analysis, now with view and context, we found that 21.8% (±5.5% CIs) of HPC units were selective for at least one factor (Figure 6b upper). 89.4% (±8.8% CIs) were selective for virtual view and 19.2% (±11.3% CIs) were selective for context. Of these, 80.9% (±11.3% CIs) were only selective for virtual view and 10.6% (±8.8% CIs) were only selective for context. 2.1% (±4.1% CIs) show a non-interacting overlap in significance, and 6.4% (±7.0% CIs) show a significant interaction.

In the LPFC 47.5% (±3.7% CIs, Figure 6b lower) were selective for at least one factor. From the selective units 92.4% (±2.8% CIs) were selective for virtual view while 27.4% (±4.7% CIs) were selective for context texture. Broken down, 72.7% (±4.7% CIs) of units significant for virtual view only, 7.7% (±2.8% CIs) significant for context only, 7.7% (±2.8% CIs) significant for both while not interacting, and 12.1% (±3.5% CIs) show an interaction. In both HPC and LPFC there was a significantly higher percentage of units that were selective for virtual view than for context (non-overlapping 95% CIs for proportions).

4 | DISCUSSION

A main contribution of our study is to demonstrate view selectivity during virtual navigation in the HPC and LPFC of macaque monkeys. Because we used a virtual maze, the views were also virtual. Units selective for virtual views are here considered to be view cells. The views were task relevant because they contained the context cue, a potential object to navigate toward, and the space that would have to be navigated through to arrive at the object. The yield of units that were selective for two very specific views might appear surprising when examining the proportion of units described in the initial view cell papers (e.g., 6% in Rolls & O'Mara (1995) and 8% in Robertson et al. (1998)). On the other hand, our proportions are similar to those reported by Nowicka and Ringo at 23% (Nowicka & Ringo, 2000), who used a screen-based task where different objects appeared in one of five positions. The differences between studies may be due to

differences in task demands associated to specific views such as the presence of a behaviourally relevant object at the viewed site. In agreement with this hypothesis, studies in rodents have reported that both landmark and reward regions can be overrepresented by place cells (Sato et al., 2020).

A study by Wirth and colleagues (Wirth et al., 2017) tracked gaze in a virtual maze with five arms, where monkeys needed to choose the correct arm of the maze to receive a reward. They found that 28% of cells appeared to be responsive when gaze was directed to a region of the environment. However, 83% of these cells had significant overlap with the greater population of cells that were selective for a combination of location, orientation, and task period. Indeed, they showed that gaze responses on a landmark could be selective for where the animal was, and how it had arrived there. In our task, we designed two ends of the maze, and intra-maze cues were identical, while distal cues were slightly different (Figure S1). Importantly, in our task the end the maze (north vs. south) was not relevant for choosing the target disc and obtaining reward. This may explain why there were so few units that responded selectively to virtual position (north vs. south). Allocentric single cell place-selectivity has been reported in the HPC in rodent and primate studies (Courellis et al., 2019; Mao et al., 2021; O'Keefe & Nadel, 1978), but has not been reported so far in the LPFC. We found a small proportion of LPFC cells that fired differentially for the two decision locations, despite there being no difference in the task demands. Over half of these cells were also modulated by which side the monkey was looking at. Interestingly a recent study has reported that spatial position in the X-maze can be decoded from neural population activity in the LPFC of macaque monkeys (Johnston et al., 2023). This suggests that LPFC neurons also encode view or spatial information that may be available during navigation tasks.

4.1 | View and object interactions

While we have proposed that the task relevant stimulus could be driving the high number of units selective for view during the decision period, varying some task relevant parameters within the view seemed to have little effect on most of these units. Only a small portion of units were modulated by either the color or the context. Those that were selective for these variables were frequently also interacting with which side was being viewed, suggesting view is still an important factor when information is encoded in the hippocampus in a virtual environment. The fact that many of the view cells were not modulated by whether the monkey was looking at the north or the south end of the maze is likely driven by the same factor that drove results in Gulli et al. (2020) where cells were more likely to be driven by task period or position in the maze in an egocentric rather than an allocentric frame of reference. What seems relevant to the animals, at least to a larger degree, is the affordances of the view, rather than the specific visual features of the view itself. Interestingly, for the view cells described in Rolls et al. (1989) that also responded to novelty, more than half showed a significant interaction between novelty and view location. Similarly, most of the color selective units in our study showed an interaction with view, particularly in the HPC.

It is possible that some of the view related responses have to do with the walls of the maze, that limit possible locations that can be navigated to. This could relate to the existence of boundary cells measured in rodents (Alexander et al., 2020, 2023), where cells in the retrosplenial cortex responded specifically when there was a boundary object on a particular side of the animal. The foveations that we measured at the ends of the maze included the walls as well as the disc, and so could be similar. Many of the foveations that we collected in the corridor would have also contained a wall on a specific side of the animal, and there were very few cells modulated by gaze position. This suggests that at the very least what we are interpreting as view cells have more complex responses than simply looking at a boundary.

4.2 | View cells selectivity in HPC and LPFC

So far, we have not found previous studies of view cells in the LPFC of macaques. We found more units selective for eye-on-screen position during the navigation period and for view during the decision period in the LPFC relative to the HPC. The LPFC is frequently studied using retino-centric paradigms that explore attention and memory (Funahashi, 2014; Funahashi et al., 1989; Leavitt et al., 2018; Tremblay et al., 2015). However, recent reports have demonstrated that the LPFC contains neurons encoding the position of targets on the screen, even when they are not being foveated (Roussy et al., 2021; Roussy et al., 2022). View selectivity may be a manifestation of a higher-order construct where objects and background in a scene are integrated in a spatiotopic/allocentric frame in a "Gestalt" like manner.

We also found that the LPFC had a higher proportion of units that were selective for view than the HPC. However, because the HPC and LPFC experiments were conducted in different animals and the level of performance were slightly different it is difficult to arrive at firm conclusions. We consider the fact that view cells were found in both structures as probably the most interesting aspect of our results. View cells may be related to the formation of cognitive maps that guide episodic long-term memory. Interactions between the HPC and LPFC are thought to underlie episodic memory formation. Future studies should address the temporal dynamics of the information transfer between these areas.

5 | CONCLUSION

We have described view cells in the HPC and the LPFC of macaque monkeys navigating a virtual environment. A small proportion of view cells were modulated by variables such as different behaviourally relevant object features, suggesting that view selectivity may be a construct related to a "Gestalt" like perception of a scene that can serve to evaluate one's position in an environment for navigation purposes as well as contingencies of the task at hand. Importantly, our results

indicate that view cells are not exclusive to the HPC, but they may exist in an even larger proportion in executive areas of the neocortex such as the LPFC, highlighting the distributed nature of information processing underlying navigation in foveating primates.

ACKNOWLEDGMENTS

We thank B. Bally, K. Barker, J. Blonde, S. Chisling, R. Kersten, W. Kucharski, S. Nuara, and K. Thomaes for technical assistance, and all members of the JMT laboratory for support. This work was supported by the Natural Sciences and Engineering Research Council of Canada (NSERC) Postgraduate Scholarship-Doctoral Fellowship, Ontario Graduate Scholarship, The Deutsche Forschungsgemeinschaft, Jonathan & Joshua Memorial Graduate Scholarship in Mental Health Research, McGill David G. Guthrie Fellowship, and National Science Foundation (2015276). This work was further supported by the Canadian Institutes of Health Research (CIHR), NSERC, BrainsCAN, and Neuronex (ref. FL6GV84CKN57) grants to J.C.M.-T.

CONFLICT OF INTEREST STATEMENT

The authors declare no competing interests.

DATA AVAILABILITY STATEMENT

The data that support the findings of this study are available from the corresponding author upon reasonable request.

ORCID

Benjamin W. Corrigan https://orcid.org/0000-0003-2630-7919
Roberto A. Gulli https://orcid.org/0000-0001-5983-0672
Guillaume Doucet https://orcid.org/0000-0003-2260-1002
Borna Mahmoudian https://orcid.org/0000-0001-5868-1732
Mohamad Abbass https://orcid.org/0000-0003-1899-2696
Megan Roussy https://orcid.org/0000-0002-7723-883X
Rogelio Luna https://orcid.org/0000-0003-0711-7562
Adam J. Sachs https://orcid.org/0000-0002-3630-4562
Julio C. Martinez-Trujillo https://orcid.org/0000-0003-3338-578X

REFERENCES

Alexander, A. S., Carstensen, L. C., Hinman, J. R., Raudies, F., William Chapman, G., & Hasselmo, M. E. (2020). Egocentric boundary vector tuning of the retrosplenial cortex. *Science Advances*, *6*(8), eaaz2322. https://doi.org/10.1126/SCIADV.AAZ2322

Alexander, A. S., Robinson, J. C., Stern, C. E., Hasselmo, M. E. (2023). Gated transformations from egocentric to allocentric reference frames involving retrosplenial cortex, entorhinal cortex and Hippocampus. *Hippocampus*. (in press).

Blonde, J. D., Roussy, M., Luna, R., Mahmoudian, B., Gulli, R. A., Barker, K. C., Lau, J. C., & Martinez-Trujillo, J. C. (2018). Customizable cap implants for neurophysiological experimentation. *Journal of Neuroscience Methods*, *304*, 103–117. https://doi.org/10.1016/j.jneumeth.2018.04.016

Cahusac, P. M. B., Miyashita, Y., & Rolls, E. T. (1989). Responses of hippocampal formation neurons in the monkey related to delayed spatial response and object-place memory tasks. *Behavioural Brain Research*, *33*(3), 229–240. https://doi.org/10.1016/S0166-4328(89)80118-4

Corrigan, B. W., Gulli, R. A., Doucet, G., & Martinez-Trujillo, J. C. (2017). Characterizing eye movement behaviors and kinematics of non-human primates during virtual navigation tasks. *Journal of Vision*, *17*(12), 15. https://doi.org/10.1167/17.12.15

Courellis, H. S., Nummela, S. U., Metke, M., Diehl, G. W., Bussell, R., Cauwenberghs, G., & Miller, C. T. (2019). Spatial encoding in primate hippocampus during free navigation. *PLoS Biology*, *17*(12), e3000546. https://doi.org/10.1371/JOURNAL.PBIO.3000546

De Araujo, I. E. T., Rolls, E. T., & Stringer, S. M. (2001). A view model which accounts for the spatial fields of hippocampal primate spatial view cells and rat place cells. *Hippocampus*, *11*(6), 699–706. https://doi.org/10.1002/hipo.1085

Doucet, G., Gulli, R. A., Corrigan, B. W., Duong, L. R., & Martinez-Trujillo, J. C. (2020). Modulation of local field potentials and neuronal activity in primate hippocampus during saccades. *Hippocampus*, *30*(3), 192–209. https://doi.org/10.1002/hipo.23140

Feigenbaum, J. D., & Rolls, E. T. (1991). Allocentric and egocentric spatial information processing in the hippocampal formation of the behaving primate. *Psychobiology*, *19*(1), 21–40. https://doi.org/10.1007/BF03337953

Funahashi, S. (2014). Saccade-related activity in the prefrontal cortex: Its role in eye movement control and cognitive functions. *Frontiers in Integrative Neuroscience*, *8*(JUNE), 54. https://doi.org/10.3389/fnint.2014.00054

Funahashi, S., Bruce, C. J., & Goldman-Rakic, P. S. (1989). Mnemonic coding of visual space in the monkey's dorsolateral prefrontal cortex. *Journal of Neurophysiology*, *61*(2), 331–349. https://doi.org/10.1152/jn.1989.61.2.331

Furuya, Y., Matsumoto, J., Hori, E., Boas, C. V., Tran, A. H., Shimada, Y., Ono, T., & Nishijo, H. (2014). Place-related neuronal activity in the monkey parahippocampal gyrus and hippocampal formation during virtual navigation. *Hippocampus*, *24*(1), 113–130. https://doi.org/10.1002/hipo.22209

Georges-François, P., Rolls, E. T., & Robertson, R. G. (1999). Spatial view cells in the primate hippocampus: Allocentric view not head direction or eye position or place. *Cerebral Cortex*, *9*(3), 197–212. https://doi.org/10.1093/cercor/9.3.197

Gulli, R. A., Duong, L. R., Corrigan, B. W., Doucet, G., Williams, S., Fusi, S., & Martinez-Trujillo, J. C. (2020). Context-dependent representations of objects and space in the primate hippocampus during virtual navigation. *Nature Neuroscience*, *23*(1), 103–112. https://doi.org/10.1038/s41593-019-0548-3

Hori, E., Nishio, Y., Kazui, K., Umeno, K., Tabuchi, E., Sasaki, K., Endo, S., Ono, T., & Nishijo, H. (2005). Place-related neural responses in the monkey hippocampal formation in a virtual space. *Hippocampus*, *15*(8), 991–996. https://doi.org/10.1002/hipo.20108

Johnston, R., Abbass, M., Corrigan, B., Gulli, R. A., Martinez-Trujillo, J., & Sachs, A. (2023). Decoding spatial locations from primate lateral prefrontal cortex neural activity during virtual navigation. *Journal of Neural Engineering*, *20*, 16054. https://doi.org/10.1088/1741-2552/ACB5C2

Leavitt, M. L., Pieper, F., Sachs, A. J., & Martinez-Trujillo, J. C. (2018). A quadrantic bias in prefrontal representation of visual-mnemonic space. *Cerebral Cortex*, *28*(7), 2405–2421. https://doi.org/10.1093/cercor/bhx142

Mao, D., Avila, E., Caziot, B., Laurens, J., Dickman, J. D., & Angelaki, D. E. (2021). Spatial modulation of hippocampal activity in freely moving macaques. *Neuron*, *109*(21), 3521–3534.e6. https://doi.org/10.1016/J.NEURON.2021.09.032

Miller, J. F., Neufang, M., Solway, A., Brandt, A., Trippel, M., Mader, I., Hefft, S., Merkow, M., Polyn, S. M., Jacobs, J., Kahana, M. J., & Schulze-Bonhage, A. (2013). Neural activity in human hippocampal formation reveals the spatial context of retrieved memories. *Science*, *342*(6162), 1111–1114. https://doi.org/10.1126/science.1244056

Nowicka, A., & Ringo, J. L. (2000). Eye position-sensitive units in hippocampal formation and in inferotemporal cortex of the macaque monkey. *The European Journal of Neuroscience*, *12*(2), 751–759.

O'Keefe, J., & Nadel, L. (1978). *The hippocampus as a cognitive map*. Oxford University Press.

Ono, T., Nakamura, K., Nishijo, H., & Eifuku, S. (1993). Monkey hippocampal neurons related to spatial and nonspatial functions. *Journal of Neurophysiology*, *70*(4), 1516–1529. https://doi.org/10.1152/jn.1993.70.4.1516

Robertson, R. G., Rolls, E. T., & Georges-François, P. (1998). Spatial view cells in the primate hippocampus: Effects of removal of view details. *Journal of Neurophysiology*, *79*(3), 1145–1156. https://doi.org/10.1152/jn.1998.79.3.1145

Rolls, E. T., Miyashita, Y., Cahusac, P. M. B., Kesner, R. P., Niki, H., Feigenbaum, J. D., & Bach, L. (1989). Hippocampal neurons in the monkey with activity related to the place in which a stimulus is shown. *Journal of Neuroscience*, *9*(6), 1835–1845. https://doi.org/10.1523/jneurosci.09-06-01835.1989

Rolls, E. T. (2023). Hippocampal spatial view cells for memory and navigation, and their underlying connectivity in humans. *Hippocampus*, *33*, 533–572. https://doi.org/10.1002/HIPO.23467

Rolls, E. T., & O'Mara, S. M. (1995). View-responsive neurons in the primate hippocampal complex. *Hippocampus*, *5*(5), 409–424. https://doi.org/10.1002/hipo.450050504

Rolls, E. T., Treves, A., Robertson, R. G., Georges-François, P., & Panzeri, S. (1998). Information about spatial view in an ensemble of primate hippocampal cells. *Journal of Neurophysiology*, *79*(4), 1797–1813. https://doi.org/10.1152/JN.1998.79.4.1797/ASSET/IMAGES/LARGE/JNP.AP34F11.JPEG

Roussy, M., Corrigan, B., Luna, R., Gulli, R. A., Sachs, A. J., Palaniyappan, L., & Martinez-Trujillo, J. C. (2022). Stable working memory and perceptual representations in macaque lateral prefrontal cortex during naturalistic vision. *The Journal of Neuroscience*, *42*(44), JN-RM-0597-22. https://doi.org/10.1523/JNEUROSCI.0597-22.2022

Roussy, M., Luna, R., Duong, L., Corrigan, B., Gulli, R. A., Nogueira, R., Moreno-Bote, R., Sachs, A. J., Palaniyappan, L., & Martinez-Trujillo, J. C. (2021). Ketamine disrupts naturalistic coding of working memory in primate lateral prefrontal cortex networks. *Molecular Psychiatry*, *26*(11), 6688–6703. https://doi.org/10.1038/s41380-021-01082-5

Sato, M., Mizuta, K., Islam, T., Kawano, M., Sekine, Y., Takekawa, T., Gomez-Dominguez, D., Schmidt, A., Wolf, F., Yamakawa, H., Ohkura, M., Lee, M. G., Fukai, T., Nakai, J., & Hayashi, Y. (2020). Distinct mechanisms of over-representation of landmarks and rewards in the hippocampus. *Cell Reports*, *32*(1), 107864. https://doi.org/10.1016/j.celrep.2020.107864

Sato, N., Sakata, H., Tanaka, Y., & Taira, M. (2004). Navigation in virtual environment by the macaque monkey. *Behavioural Brain Research*, *153*(1), 287–291. https://doi.org/10.1016/J.BBR.2003.10.026

Smith, A. C., Frank, L. M., Wirth, S., Yanike, M., Hu, D., Kubota, Y., Hu, D., Kubota, Y., Graybiel, A. M., Suzuki, W. A., & Brown, E. N. (2004). Dynamic analysis of learning in behavioral experiments. *Journal of Neuroscience*, *24*(2), 447–461. https://doi.org/10.1523/JNEUROSCI.2908-03.2004

Tamura, R., Ono, T., Fukuda, M., & Nakamura, K. (1990). Recognition of egocentric and allocentric visual and auditory space by neurons in the hippocampus of monkeys. *Neuroscience Letters*, *109*(3), 293–298. https://doi.org/10.1016/0304-3940(90)90010-7

Tamura, R., Ono, T., Fukuda, M., & Nakamura, K. (1992). Spatial responsiveness of monkey hippocampal neurons to various visual and auditory stimuli. *Hippocampus*, *2*(3), 307–322. https://doi.org/10.1002/hipo.450020309

Tremblay, S., Pieper, F., Sachs, A., & Martinez-Trujillo, J. (2015). Attentional filtering of visual information by neuronal ensembles in the primate lateral prefrontal cortex. *Neuron*, *85*(1), 202–215. https://doi.org/10.1016/j.neuron.2014.11.021

Wirth, S., Baraduc, P., Planté, A., Pinède, S., & Duhamel, J.-R. (2017). Gaze-informed, task-situated representation of space in primate hippocampus during virtual navigation. *PLoS Biology*, *15*(2), e2001045. https://doi.org/10.1371/journal.pbio.2001045

SUPPORTING INFORMATION

Additional supporting information can be found online in the Supporting Information section at the end of this article.

How to cite this article: Corrigan, B. W., Gulli, R. A., Doucet, G., Mahmoudian, B., Abbass, M., Roussy, M., Luna, R., Sachs, A. J., & Martinez-Trujillo, J. C. (2023). View cells in the hippocampus and prefrontal cortex of macaques during virtual navigation. *Hippocampus*, *33*(5), 573–585. https://doi.org/10.1002/hipo.23534